Examination of milled h-BN addition on sintered Si_3N_4/h-BN ceramic composites

Katalin Balázsi, Mónika Furko*, Zsolt Fogarassy, Csaba Balázsi

Centre for Energy Research, Hungarian Academy of Sciences, Konkoly-Thege M. str. 29-33, Budapest, Hungary

Abstract

Silicon nitride (Si_3N_4) ceramics containing 1 and 5 wt.% of hexagonal boron nitride (h-BN) were prepared by attrition milling and hot-isostatic pressing. Thorough morphological characterizations have been carried out to reveal the influence of the milling parameters on the size of the h-BN additives. The results confirmed significant decrease in h-BN particle size by increasing milling time. The transmission electron microscopy observations revealed that the h-BN particles were incorporated into the ceramic matrix. The results showed that the increase of the h-BN content decreased significantly the hardness of materials. Moreover, the hardness values were higher when the size of h-BN was larger. The same tendency was observed in the case of Young's modulus.

Keywords: *Si_3N_4, h-BN, milling, hot pressing, structure, mechanical properties*

I. Introduction

Silicon nitride (Si_3N_4) and boron nitride (BN) are both important ceramics for engineering applications. They are characterized by high temperature resistance and chemical stability [1,2]. In addition, it has been reported that the plate-like hexagonal boron nitride (h-BN) can enhance the machinability of the Si_3N_4/h-BN composites if the h-BN content is high enough [3–6]. The good machinability is very important issue in the industrial application, because the extreme hardness of these ceramics makes the conventional machining very difficult and expensive [7–11]. In addition, Si_3N_4-based ceramics are potential substitutes for commonly used materials for devices operating under extreme conditions (high temperature, vacuum) [12,13], owing to their high hardness and mechanical stability under a broad range of temperatures, low density, low thermal expansion and high specific stiffness [14].

The tribological performance of ceramics can be further enhanced by incorporation of solid lubricants into the matrix material [15–17]. Hexagonal BN is a potential lubricating agent [18–20] with beneficial effect on the tribological performance of Si_3N_4/BN composites at room temperature, by reducing the wear coefficient by one order of magnitude, compared to the matrix material [19]. The friction coefficient of composites also decreases [19]. Skoop *et al.* [18] found that the tribological parameters were independent on the sliding speed and BN content. At elevated temperatures (300 °C) BN starts to oxidise, hindering the lubricating role of the dispersion. The tribological performance of Si_3N_4/BN composites against a steel counterface showed that the BN addition had no considerable effect on the friction and wear coefficients [16]. In this case, BN was reported to be ineffective in providing a solid lubricating film at room temperature. A comparison of the sliding wear behaviour of monolithic Si_3N_4 and Si_3N_4/BN composites in aqueous environment revealed a slight increase in the wear coefficient with BN additions up to 70 wt.% [17]. The steady-state friction values showed no direct dependence on the BN content. Carrapichano *et al.* [21] stated that the addition of boron nitride platelets improved their tribological properties only if low volume amounts (10 vol.%) were incorporated. It is also reported that the fracture strength of Si_3N_4/h-BN ceramics remarkably decreased with increasing the BN content because of the aggregation of h-BN flakes [22].

The Si_3N_4/h-BN composites can be prepared by various processing methods such as hot-pressing sinter-

ing [6,23], reactive pressureless sintering [24], chemical synthesis methods using BN precursor [3,4,25] and gel casting [22]. Gel casting is well-established to fabricate homogeneous, complex-shaped and machinable green body at low cost in last decades [26–29]. Wang *et al.* [30] prepared porous Si_3N_4/BN composite ceramics with homogeneous dispersion of BN by the gel casting technique. They found that with increasing BN content, the mechanical properties of porous Si_3N_4/BN ceramics partially worsened, but the dielectric properties and thermal shock resistance had been improved [30]. The Si_3N_4/h-BN composites can also be hot pressed via chemical method in order to homogeneously disperse h-BN powders in Si_3N_4 matrix [3–6] because of the poor sinterability of h-BN. The poor sinterability of h-BN comes from its strong covalent nature and plate-like structure [31]. Li *et al.* [6] fabricated Si_3N_4/BN composites by spark plasma sintering (SPS) through traditional powder mixing process and by chemical route. The SPS-processed Si_3N_4/BN materials showed high bending strength compared to composites obtained by chemical procedure. The microstructures of the produced Si_3N_4-based ceramics could be tailored by combining the SPS technique with a rapid heating time [32]. Industrial applications of Si_3N_4/BN ceramics are still limited because of the complicated preparation process and expensive production cost [22]. It can be stated that until now preparing Si_3N_4/h-BN composites using mechanical mixture and then hot isostatic pressing method are rarely discussed as well as there are no detailed reports on the dependence of microstructure and BN particle size on the milling conditions [33–35].

To the best of our knowledge, there is no published scientific report that examined the effect of different milling conditions as well as h-BN content on the microstructure and sinterability of Si_3N_4/h-BN composite materials. Our study aims to give a deep insight into the form and size and position of BN additives within the silicon nitride matrix. We also investigated the correlation between the size of h-BN particles and the mechanical properties of composite matrices.

In this work, silicon nitride composites with different percentage of h-BN were prepared by hot isostatic pressing. Three types of Si_3N_4/h-BN composite preparation methods were assessed. The effect of h-BN content on the microstructure and mechanical properties of Si_3N_4/h-BN ceramics was evaluated and discussed.

II. Experimental

2.1. Powder mixture preparation

The nanosized h-BN powders were prepared by mechanical milling using commercial BN powder (hexagonal, 99.99%, average diameter of 3–4 μm, H.C. Starck). The powders were milled in high-efficient attrition mill (Union Process, 01-HD/HDDM) equipped with zirconia agitator delta discs (with diameter of 1 mm) and zirconia grinding media in a 750 cm³ zirconia tank. The milling was carried out in 96% ethanol at 4000 rpm for 10 h. After wet milling, dry milling was also performed at 4000 rpm for 5 h.

The h-BN powder was mixed with a Si_3N_4 powder mixture containing 90 wt.% Si_3N_4, 4 wt.% Al_2O_3 and 6 wt.% Y_2O_3. The composite powder mixtures containing 1 and 5 wt.% h-BN were prepared by three different methods. In the first method, the h-BN particles were added to the Si_3N_4 powder mixture without pre-milling. The Si_3N_4 powder mixture and h-BN powder (1 and 5 wt.%) were milled for 5 hours at 4000 rpm in distilled water (samples B1/1 and B1/5, respectively). In the second method, the Si_3N_4 powder mixture was first milled for 4.5 h at 4000 rpm in distilled water and then the nano-sized, pre-milled h-BN particles were added to the base composite and milled together for 0.5 h at 600 rpm (samples C2/1 and C2/5). While in the third method, the pre-milled h-BN powder was added to the Si_3N_4 matrix at the beginning of milling, the milling procedure of this mixture also lasted for 5 hours at 4000 rpm in distilled water (samples D3/1 and D3/5). Such prepared powders were then dried and sieved with a filter with mesh size of 150 μm. The h-BN particles were added as lubricating agent for ceramic matrices. The composition of samples and detailed preparation conditions are presented in Table 1.

2.2. Hot isostatic pressing (HIP)

After the high-energy milling, hot isostatic pressing was performed as sintering method for composites. Before HIP (ABRA AG HIP), the Si_3N_4/h-BN composite samples were oxidized at 400 °C to evaporate the polyethylene glycol (PEG). The PEG was added to the powder mixture to aid the dry pressing of composite in volume ratio of 10%. The heating rate was 25 °C/min. The HIP was carried out at 1700 °C in high purity nitrogen atmosphere using BN embedding powder at 20 MPa for 3 h.

Table 1. Detailed preparation methods of Si_3N_4/h-BN composite powder mixtures

| Samples	h-BN amount [wt.%]	Mixing conditions	Milling parameters
B1/1	1	un-milled h-BN particles added to Si_3N_4	5 h, 4000 rpm, H_2O
B1/5	5	base powder mixture	
C2/1	1	pre-milled h-BN particles added to Si_3N_4 base	I) 4.5 h, 4000 rpm, H_2O
C2/5	5	powder mixture 0.5 h before the end of milling	II) 0.5 h, 600 rpm, H_2O
D3/1	1	pre-milled h-BN particles added to Si_3N_4 base	5 h, 4000 rpm, H_2O
D3/5	5	powder mixture at the beginning of milling	
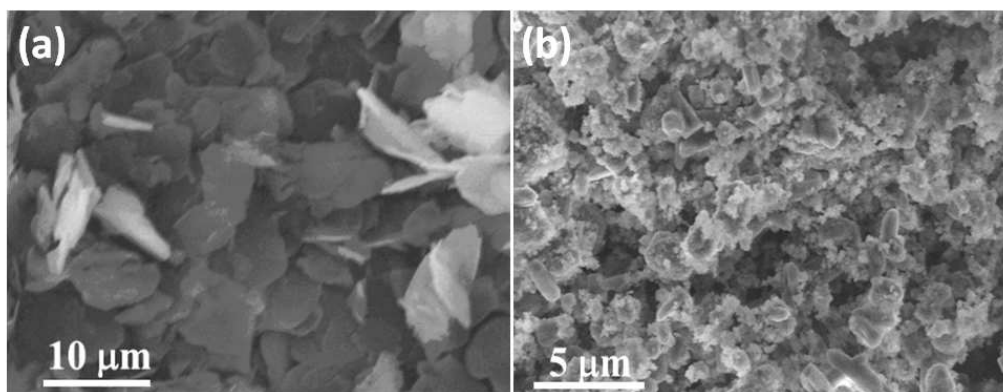
Figure 1. SEM images of h-BN before (a) and after milling (b)

2.3. Characterization techniques

SEM studies of the prepared samples were performed with LEO 1540XB Crossbeam workstation. The beam parameters in SEM imaging mode were 5 keV beam energy and 30 μm aperture size. Everhart-Thornley and In-Lens secondary electron detectors were used. For SEM observations, the samples were tilted at angle of 36°. The electron beam parameters for the EDX were 8 keV beam energy. A Röntec Si(Li) detector and the Bruker Esprit 1.9 software had been used for the EDX measurements. TEM measurements were performed to study the structural properties of investigated samples (TEM, Philips CM-20) with accelerating voltage of 200 kV. All composites were initially mechanically thinned to ~50 μm, and then further thinned till perforation by 6 kV Ar^+ ions from both sides. The thinning and cleaning of the TEM samples was accomplished by 2 keV Ar^+ ions. This procedure minimized the thermal shock during sample preparation for TEM. Phase compositions were determined by X-ray diffractometer. XRD diffractograms were recorded at room temperature by Bruker AXS D8 diffractometer (Cu K_α radiation source, 0.15418 nm) equipped with Göbel mirror and GADDS 2D detector system operating at 40 kV and 40 mA. The diffraction patterns were collected over a 2θ range from 20° to 90° with 1°/min steps using flat plane geometry.

Hardness of the composites was determined by Vickers indentation (hardness testers LECO 700AT) under load of 10 N, the dwelling time was 10 s in all cases. Young's modulus was measured by four point bending method on specimens with dimensions $3 \times 4 \times 50$ mm. The surfaces of samples were thoroughly polished down to surface roughness below 0.05 μm.

The densities of the sintered specimens were measured according to Archimedes' principle. Sintered specimens were cut, polished to 1 μm finish by routine ceramography procedure.

III. Results and discussion

3.1. Morphology of h-BN powder

Lamellar morphology of the starting h-BN powder with average diameter of 4–10 μm and submicron thickness is revealed by SEM investigation (Fig. 1a). The intensive wet milling in 96% ethanol at 4000 rpm for 10 h and consecutive dry milling at 4000 rpm for 5 h resulted in a bimodal grain size of the h-BN powder (Fig. 1b). The resulting h-BN powder consists of grains in submicron range and larger grains with 2–4 μm in length.

3.2. Morphology of Si₃N₄/h-BN powders and ceramics

Morphological investigations were taken on the powder mixtures prepared by different methods before and after HIP treatment to study the morphology of particles and surface of the composites.

The morphological investigations confirmed that the ceramic-mixture powders are very similar in all cases. They consist of mainly small, sub-micron sized particles and larger agglomerates. Only in the case of h-BN particles added to the Si_3N_4 base powder mixture without pre-milling the stand-alone h-BN particles (white arrows) can be observed in both samples with 1 and 5 wt.% h-BN (Figs. 2a and 2c). The pre-milled h-BN particles added to the Si_3N_4 base powder mixture 0.5 h before the end of milling (Figs. 3a and 3c) and pre-milled h-BN particles added to the Si_3N_4 base powder mixture at the beginning of milling (Figs. 4a and 4c) showed similar features, namely the same submicron particles in each case, at 1 or 5 wt.% h-BN addition as well.

The sintered samples, on the other hand, showed smoother and more homogeneous surface, but cracks and a few large, micron-sized particles are also visible. The surface morphologies of the B1/1 and B1/5 samples (Figs. 2b and 2d) demonstrate different characteristics. In these cases, the particles are more distinct and rod-like particles are also present along with rounded particles.

In addition, it is also visible that the surface of the sintered D3/1 and D3/5 samples (Figs. 4b and 4d) is more homogeneous and dense than the surface of other samples (B1 and C2). This proves that increase in the milling time of h-BN can improve the sinterability of materials.

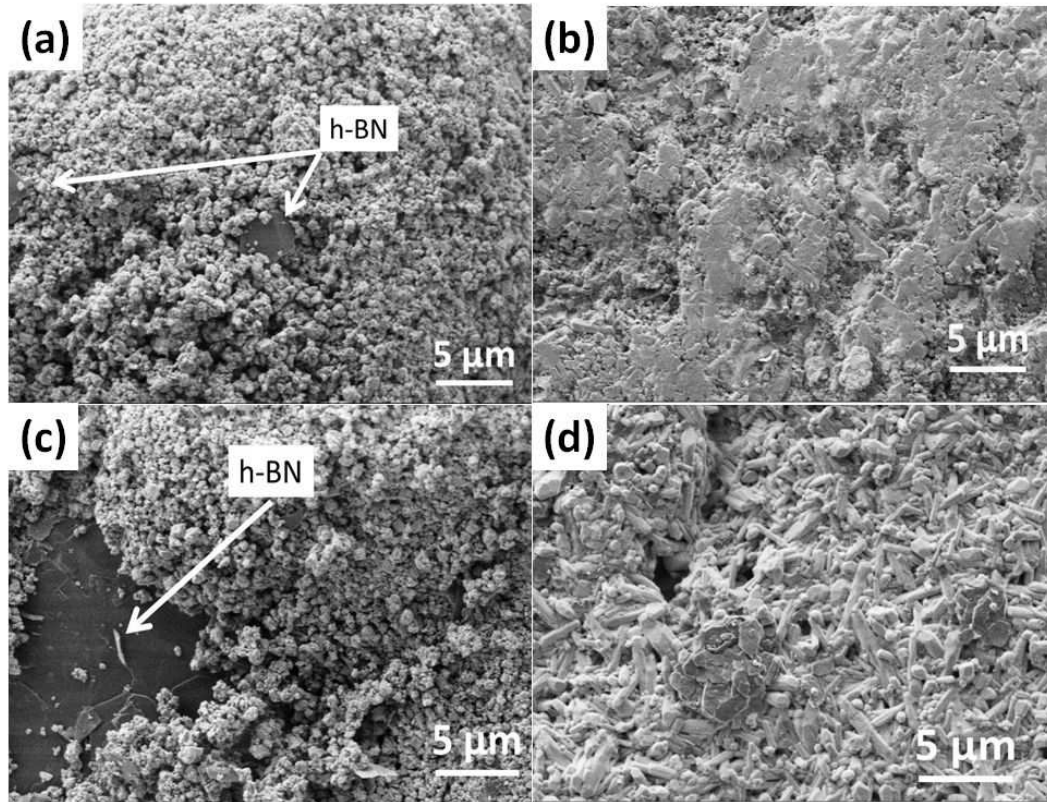The densities of samples are summarized in Table 2.

Figure 2. SEM images of B1 samples - powder mixtures (a,c) and sintered samples (b,d) with un-milled h-BN particles added to the Si₃N₄ base powder: 1 wt.% h-BN (a,b) and 5 wt.% h-BN (c,d)
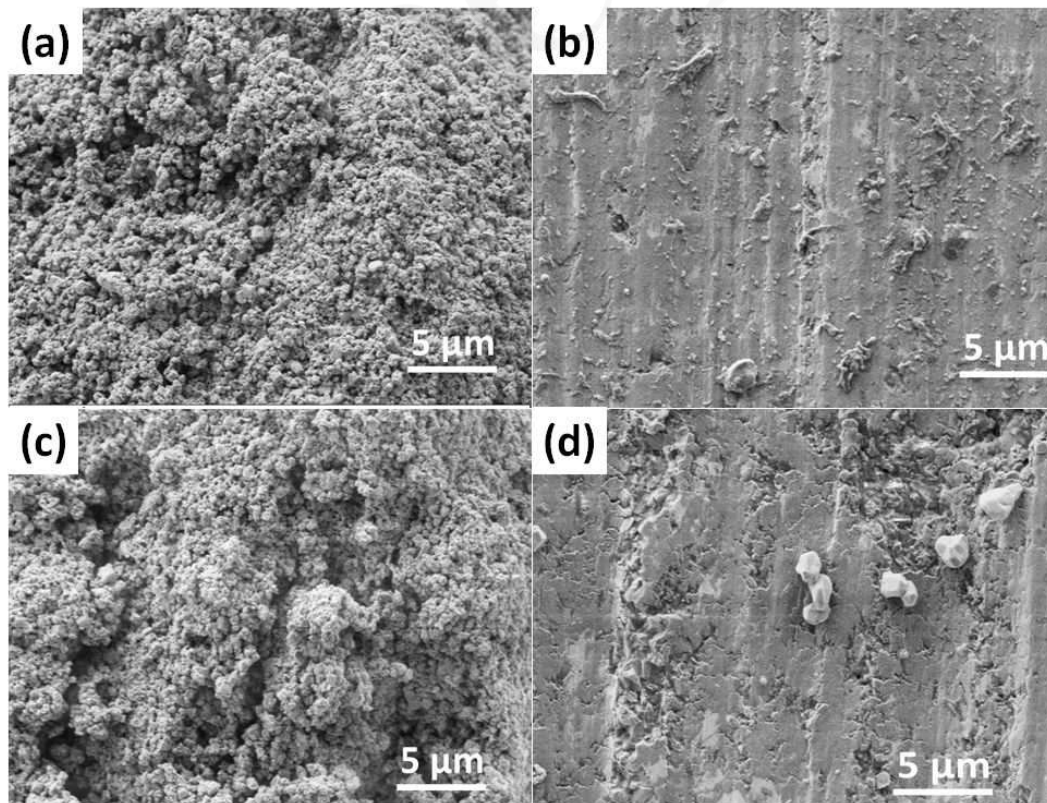

Figure 3. SEM images of C2 samples - powder mixtures (a,c) and sintered samples (b,d) with pre-milled h-BN particles added to the Si₃N₄ base powder 0.5 h before the end of milling: 1 wt.% h-BN (a,b) and 5 wt.% h-BN (c,d)
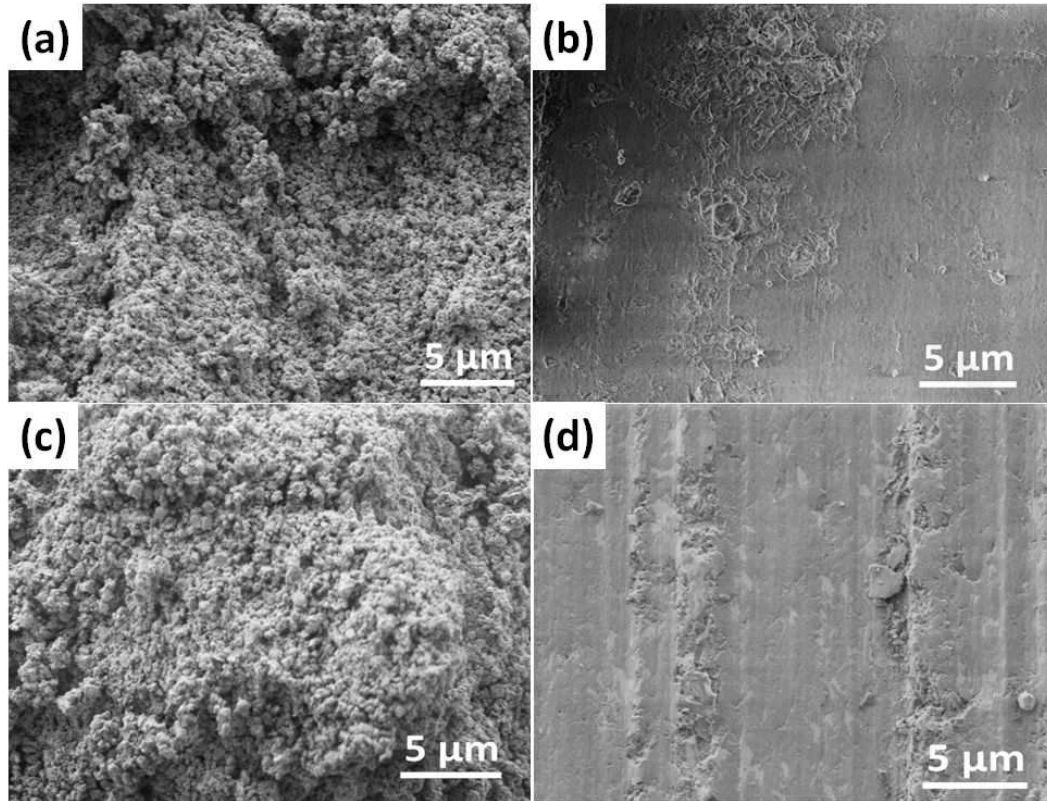
Figure 4. SEM images of D3 samples - powder mixtures (a,c) and sintered samples (b,d) with pre-milled h-BN particles added to the Si₃N₄ base powder at the beginning of milling: 1 wt.% h-BN (a,b) and 5 wt.% h-BN (c,d)

Table 2. Densities of investigated h-BN/Si₃N₄ samples

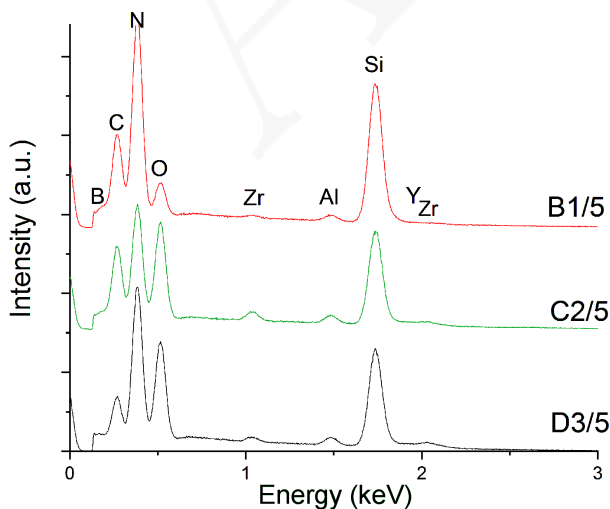| Samples	Density [g/cm³]
B1/1	3.35
B1/5	3.245
C2/1	3.375
C2/5	3.060
D3/1	3.376
D3/5	3.165

Figure 5. EDX of Si₃N₄/h-BN samples containing 5 wt.% boron nitride additives

It is visible that the densities of the samples are very similar and the different milling conditions have no effect on their values. On the other hand, the higher h-BN content decreased the densities of samples prepared with different methods.

Figure 5 shows the detectable elements in the samples prepared by different milling conditions. It is visible that all spectra are very similar and the samples contain large amount of Si, N, O and C elements. In addition, weak peaks of B, Zr and Al peaks are also detected. The Zr contamination came from the zirconia grinding media and C from carbon tape used in the EDX investigation.

3.3. Structure of powders and composites

The exact structure of different particles in composite mixtures was further examined by TEM measurements. The images demonstrate that scattered h-BN platelets can be found amongst the Si₃N₄ ceramic particles in all samples. The diameter of Si₃N₄ particles varied between 300 and 1000 nm. There was no distinct difference among the structures of the samples differing only in the h-BN additive content. On the other hand, the different milling conditions caused significant change in the size and structure of h-BN additives. The micro-sized h-BN platelets became disintegrated by increasing the extent of milling, as it is visible in the bright-field (BF) TEM images (Fig. 6). The largest h-BN particles were in the B1 samples prepared without pre-milling. The size of particles changed between 5 and 9 μm in length and 400–1000 nm in thickness. Application of
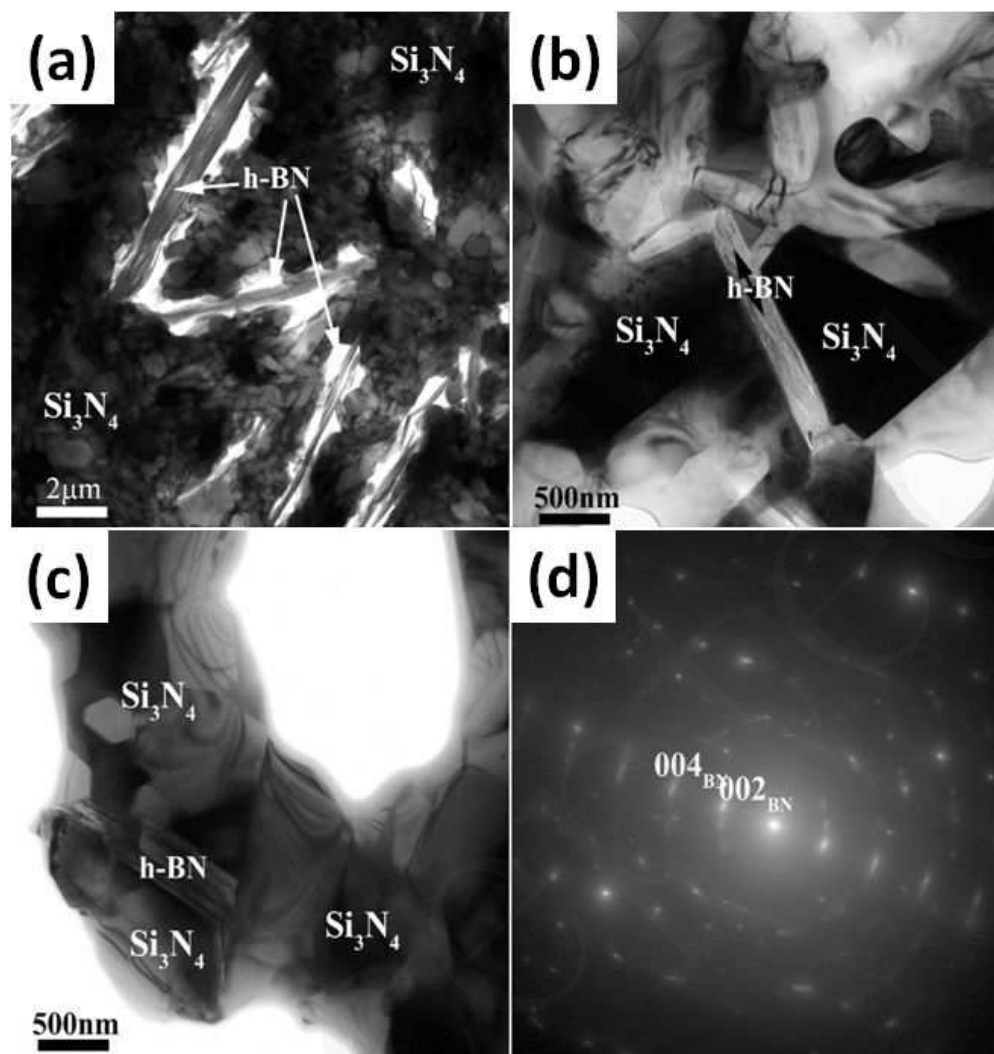
361

Figure 6. Bright-field TEM images of samples: a) B1/5, b) C2/1 and c) D3/1 as well as SAED on one h-BN platelet within the B1/5 sample (d)

pre-milling procedure decreased the size of the h-BN particles by around 65–85%. In this case the size of the particles was only 0.5–2 μm in length and their thickness varied between 100 and 350 nm. However, it did not cause any measurable change in the size of h-BN platelets when they were mixed with the Si_3N_4 base ceramics at the beginning or 0.5 h before the end of milling procedure (the D3 samples).

The BF-TEM images with higher magnifications (Fig. 7) clearly demonstrate that the h-BN platelets are present in the matrix as thin and almost parallel aggregated plate-like particles. The thickness of these plate-like particles in the samples prepared without pre-milling (B1) was 5–100 nm, while in the case of pre-milled particles (C2 and D3) the thickness was changed between 5 and 25 nm.

The h-BN particles can be clearly distinguished from the main matrix on TEM images (Fig. 7) owing to their different form. Moreover, in the selected area electron diffraction pattern, their exact structure was also easily identifiable.

3.4. XRD measurements

Figures 8a and 8b demonstrate the XRD patterns of Si_3N_4/h-BN ceramic composites containing 1 and 5 wt.% h-BN, respectively. The XRD results indicated that the main phase in all composite mixtures is β-Si_3N_4. The main peaks of β-Si_3N_4 phase (JCPDS 83-0701) can be identified at $2\theta = 13.2°$, $23.1°$, $26.7°$ and $33.6°$ with the highest intensity at $26.7°$. However, there is no visible peak of the h-BN phase in all spectra. Two main characteristic peaks of h-BN phase are at $2\theta = 13.2°$ and $26.6°$ according to PDF database file #74-1978. The absence of these distinct characteristic peaks of h-BN phase can be explained by their merging with the reflections of β-Si_3N_4 phase appearing at similar 2θ values. This assumption can be related to the difference in intensity of the characteristic peak at $26.6°$, which is the highest in the cases when the h-BN particles were added to the matrix composite without pre-milling. This means that the measured intensity of characteristic peaks increased with the size of h-BN particles. Each sample contained also some zirconia as contamination
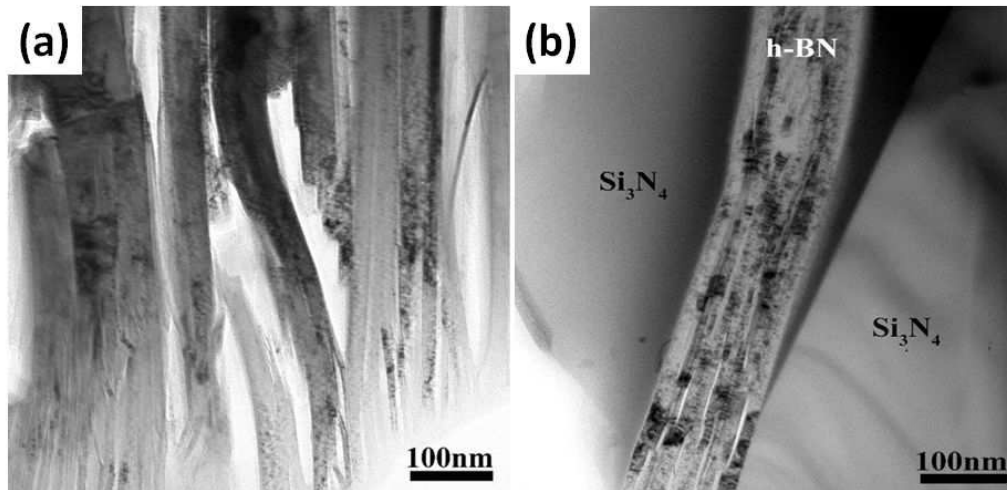
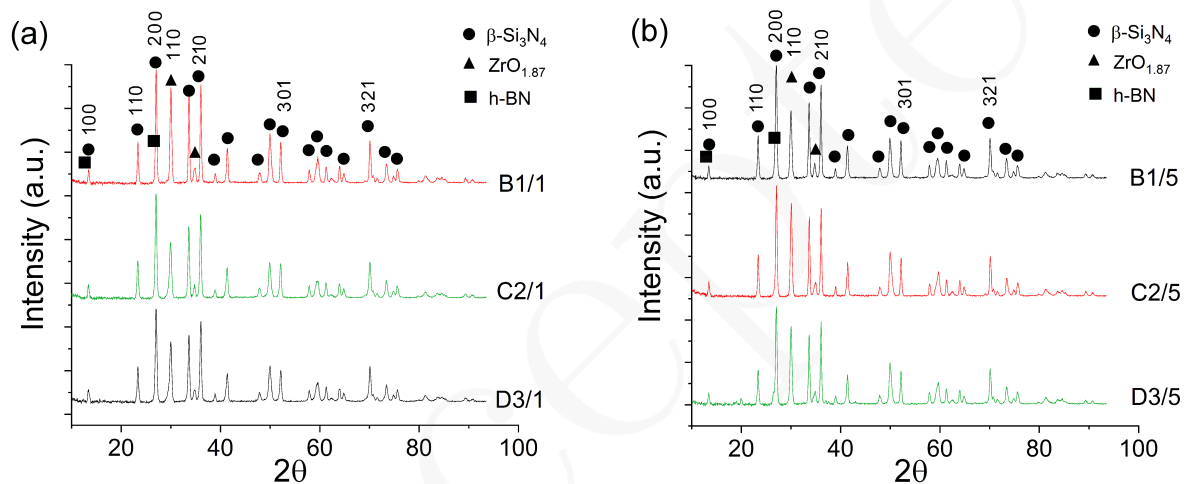**Figure 7. BF-TEM images on h-BN platelets: a) sample B1/5 and (b) sample D3/1**

Figure 8. XRD patterns of Si$_3$N$_4$-based composites with: a) 1 wt.% and b) 5 wt.% h-BN, prepared by different procedures

after intensive milling in ZrO_2 medium before sintering. The main characteristic peak of identified $ZrO_{1.87}$ phase (JCPDS 81-1551) appears at $2\theta = 30.0°$ in all spectra.

3.5. Mechanical properties

Figure 9 shows the changes in the hardness of the Si$_3$N$_4$/h-BN composites both with milling conditions and with BN content. The Vickers hardness of β-Si$_3$N$_4$ base ceramics was 16.4 GPa [33]. It is visible that the hardness of the composites is lower than the hardness of the monolithic β-Si$_3$N$_4$. Moreover, the hardness of the composites largely decreased with increasing h-BN content. The milling conditions, i.e. the sizes of h-BN additives, has also affected the hardness of composite materials. The hardness values of the composites, prepared by the first method and containing the largest, micro-sized h-BN particles were the highest, and the hardness slightly decreased when the size of h-BN particles was smaller. The lower hardness of the composites compared to the monolithic material is also due to the porosity remaining in the material after sintering [33]. Moreover, it is reported that the easy cleavage of basal

plane of h-BN platelets causes decrease in the hardness with h-BN addition [11].

In practice, Young's modulus is used to measure the stiffness of different solid materials and it can also de-
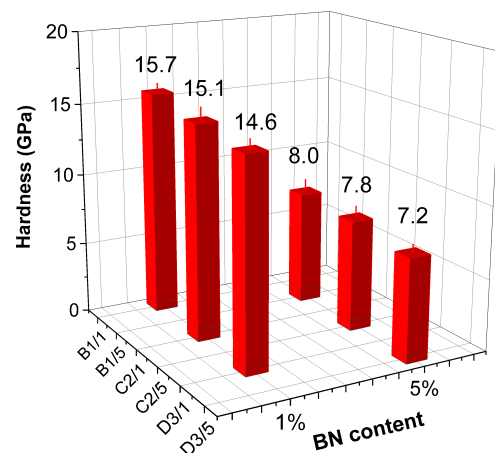

Figure 9. Hardness of Si$_3$N$_4$/h-BN composite samples containing 1 and 5 wt.% h-BN additives prepared by different methods
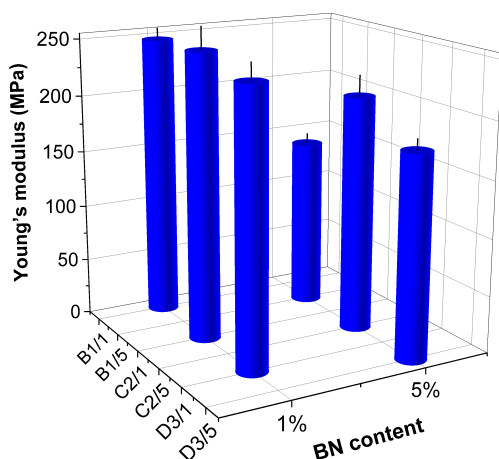
Figure 10. Young's modulus of h-BN/Si$_3$N$_4$ composite samples containing 1 and 5 wt.% h-BN additives prepared by different methods

termine their mechanical properties. As it can be seen in Fig. 10, the Young's modulus of the Si$_3$N$_4$/h-BN composites decreased with increasing BN content. On the other hand, the milling conditions (or the size of added h-BN particles) had no significant influence on the Young's modulus.

It is also confirmed that an increase in materials' porosity leads to a decrease in Young's modulus. Moreover, BN also has low Young's modulus (33.86 GPa, in the *c* direction and 85.95 GPa in the *a* direction) [36].

IV. Conclusions

Si$_3$N$_4$/h-BN composites have been prepared by three different milling procedures. Thorough morphological characterizations have been carried out to reveal the influence of the milling parameters on the size of the h-BN additives. The results confirmed significant decrease in the h-BN particle size by increasing milling time.

The BF-TEM images proved that the h-BN platelets were present in the matrix as thin and almost parallel aggregated plate-like particles. The h-BN particles could be clearly distinguished from the main matrix owing to their different form.

According to the XRD measurements, the main phases in all samples are β-Si$_3$N$_4$. In addition, BN and ZrO$_{1.87}$ phases are detected. The mechanical measurements showed that the increase of the h-BN content decreased both the hardness and Young's modulus of all the samples. In addition, the increase in the size of h-BN particles caused also increase in the hardness and Young's modulus.

ditions. Thanks to Mr. V. Varga, Mr. L. Illés and Dr. Z.E. Horváth from MTA-EK for sample preparation, performing SEM, EDS and XRD measurements.

References

1. J. Eichler, C. Lesniak, "Boron nitride (BN) and BN composites for high-temperature applications", *J. Eur. Ceram. Soc.*, **28** (2008) 1105–1109.
2. F.L. Riley, "Silicon nitride and related materials", *J. Am. Ceram. Soc.*, **83** (2000) 245–265.
3. T. Kusunose, T. Sekino, Y.H Choa, K. Niihara, "Fabrication and microstructure of silicon nitride/boron nitride nanocomposites", *J. Am. Ceram. Soc.*, **85** (2002) 2678–2688.
4. T. Kusunose, T. Sekino, Y.H. Choa, K. Niihara, "Machinability of silicon nitride/boron nitride nanocomposites", *J. Am. Ceram. Soc.*, **85** (2002) 2689–2695.
5. L. Gao, X.H. Hai, J.G. Li, Y.G. Li, J. Sun, "BN/Si$_3$N$_4$ nanocomposite with high strength and good machinability", *Mater. Sci. Eng. A*, **415** (2006) 145–148.
6. Y.L. Li, R.X. Li, J.X. Zhang, "Enhanced mechanical properties of machinable Si$_3$N$_4$/BN composites by spark plasma sintering", *Mater. Sci. Eng. A*, **483-484** (2008) 207–210.
7. D.G. Grossman, "Machinable glass-ceramics based on tetrasilicic mica", *J. Am. Ceram. Soc.*, **55** (1972) 446–449.
8. M.W. Barsoum, T. El-Raghy, "Synthesis and characterization of a remarkable ceramic: Ti$_3$SiC$_2$", *J. Am. Ceram. Soc.*, **79** (1996) 1953–1956.
9. N.P. Padture, C.J. Evans, H.H.K. Xu, B.R. Lawn, "Enhanced machinability of silicon carbide via microstructural design", *J. Am. Ceram. Soc.*, **78** (1995) 215–217.
10. K. Chihiro, Y. Akira, "Machinability of high-strength porous silicon nitride ceramics", *J. Ceram. Soc. Jap.*, **106** (1998) 1135–1137.
11. W. Ruigang, P. Wei, J. Mengning, C. Jian, L. Yongming, "Investigation of the physical and mechanical properties of hot-pressed machinable Si$_3$N$_4$/h-BN composites and FGM", *Mater. Sci. Eng. B*, **90** (2002) 261–268.
12. T.H.C. Childs, A. Mimaroglu, "Sliding friction and wear up to 600 °C of high speed steels and silicon nitrides for gas turbine bearings", *Wear*, **162-164** (1993) 890–896.
13. L. Zhou, L. Fang, N.X. Wang, J.E. Zhou, "Unlubricated sliding wear mechanism of fine ceramic Si$_3$N$_4$ against high-chromium cast iron", *Tribol. Int.*, **27** [5] (1994) 349–357.
14. F.L. Riley, "Silicon nitride and related materials", *J. Am. Ceram. Soc.*, **83** [2] (2000) 245–265.
15. M. Woydt, A. Skopp, I. Dorfel, K. Witke, "Wear engineering oxides/antiwear oxides", Tribol. Trans., 42 (1999) 21–31.
16. A. Gangopadhyay, S. Jahanmir, MB Peterson, "Self-lubricating ceramic matrix composites", pp.163–197 in *Friction and Wear of Ceramics*. Ed. S. Jahanmir, Marcel Dekker, New York, 1997.
17. T. Saito, T. Hosoe, F. Honda, "Chemical wear of sintered Si$_3$N$_4$, hBN and Si$_3$N$_4$-hBN composites by water lubrication", *Wear*, **247** (2001) 223–230.
18. A. Skopp, M. Woydt, "Ceramic-ceramic composite materials with improved friction and wear properties", *Tribol. Int.*, **25** [1] (1992) 61–70.
19. A. Skopp, M. Woydt, K.H. Habig, "Tribological behav-

ior of silicon nitride materials under unlubricated sliding between 22 °C and 1000 °C", *Wear*, **181-183** (1995) 571–580.

20. T. Saito, Y. Imada, F. Honda, "Chemical influence on wear of Si_3N_4 and hBN in water", *Wear*, **236** (1999) 153–158.

21. J.M. Carrapichano, J.R. Gomes, R.F. Silva, "Tribological behaviour of Si_3N_4-BN ceramic materials, for dry sliding applications", *Wear*, **253** (2002) 1070–1076.

22. Y. Zhuang, S. Wang, D. Jia, B. Sun, Q. Li, P. Zhang, Y. Zhou, "Fabrication of gel cast BN/Si_3N_4 composite ceramics from surface-coated BN powder", *Mater. Sci. Eng. A*, **626** (2015) 27–33.

23. D.Q. Wei, Q.C. Meng, D.C. Jia, "Mechanical and tribological properties of hot-pressed h-BN/Si_3N_4 ceramic composites", *Ceram. Int.*, **32** (2006) 549–554.

24. B. Yuan, J.X. Liu, G.J. Zhang, Y.M. Kan, P.L. Wang, "Silicon nitride/boron nitride ceramic composites fabricated by reactive pressureless sintering", *Ceram. Int.*, **35** (2009) 2155–2159.

25. K. Liu, C. Zhang, B. Li, S. Wang, F. Cao, "Synthesis of porous silicon nitride-boron nitride composites by gel-casting and PIP", *J. Mater. Eng. Perform.*, **23** [8] (2014) 2829–2833.

26. O.O. Omatete, M.A. Janney, R.A. Streklow, "Gel casting: a new ceramic forming process", *Am. Ceram. Soc. Bull.*, **70** [10] (1991) 1641–1649.

27. J.L. Yang, J.L. Yu, Y. Huang, "Recent developments in gel-casting of ceramics", *J. Eur. Ceram. Soc.*, **31** (2011) 2569–2591.

28. A.C. Yong, O.O. Omatete, M.A. Janney, P.A. Menchhofer, "Gelcasting of alumina", *J. Am. Ceram. Soc.*, **74** (1991) 612–618.

29. T. Carisey, W.A. Laugier, D.G. Brandon, "Control of texture in Al_2O_3 by gel-casting", *J. Eur. Ceram. Soc.*, **15** (1995) 1–8.

30. S. Wang, D. Jia, Z. Yang, X. Duan, Z. Tian, Y. Zhou, "Effect of BN content on microstructures, mechanical and dielectric properties of porous BN/Si_3N_4 composite prepared by gel casting", *Ceram. Int.*, **39** (2013) 4231–4237.

31. Y. Li, P. Liu, X. Wang, H. Jin, J. Yanga, G. Qiao, "Interface structure and formation mechanism of BN/intergranular amorphous phase in pressureless sintered Si_3N_4/BN composites", *Scripta Mater.*, **63** (2010) 185–188.

32. Z.J. Shen, Z. Zhao, H. Peng, M. Nygren, "Formation of tough interlocking microstructures in silicon nitride ceramics by dynamic ripening", *Nature*, **417** (2002) 266–268.

33. A. Kovalcíková, J. Balko, C. Balázsi, P. Hvizdos, J. Dusza, "Influence of hBN content on mechanical and tribological properties of Si_3N_4/BN ceramic composites", *J. Eur. Ceram. Soc.*, **34** (2014) 3319–3328.

34. Y. Sun, Q. Meng, D. Jia, Ch. Guan, "Effect of hexagonal BN on the microstructure and mechanical properties of Si_3N_4 ceramics", *J. Mater. Process. Technol.*, **182** (2007) 134–138.

35. Z. Krstic, V.D. Krstic, "Young's modulus, density and phase composition of pressureless sintered self-sealed Si_3N_4/BN laminated structures", *J. Eur. Ceram. Soc.*, **28** (2008) 1723–1730.